Design of a Semi-Powered Stance-Control Swing-Assist Transfemoral Prosthesis

Lee J. T., Bartlett, H.L., and Goldfarb M., Member, IEEE

Abstract—This paper describes the design of a new type of knee prosthesis called a stance-control, swing-assist (SCSA) knee prosthesis. The device is motivated by the recognition that energetically-passive stance-controlled microprocessor-controlled knees (SCMPKs) offer many desirable characteristics, such as quiet operation, low weight, high-impedance stance support, and an inertially-driven swing-phase motion. Due to the latter, however, SCMPKs are also highly susceptible to swing-phase perturbations, which can increase the likelihood of falling. The SCSA prosthesis supplements the behavior of an SCMPK with a small motor that maintains the low output impedance of the SCMPK swing state, while adding a supplemental closed-loop controller around it. This paper elaborates upon the motivation for the SCSA prosthesis, describes the design of a prosthesis prototype, and provides human-subject testing data that demonstrates potential device benefits relative to an SCMPK during both non-perturbed and perturbed walking.

Index Terms—Transfemoral, prosthesis, microprocessor-controlled knee, MPK, biomechanics, amputation

I. INTRODUCTION

THERE are approximately 600,000 persons living in the US with major lower limb amputation [1], roughly half of whom have transfemoral amputation (TFA) [2]. The worldwide prevalence of TFA is approximately 20-30 times the US prevalence [3]. Among the implications of TFA, individuals with TFA exhibit a drastic increase in frequency of falls [4-5] and increased frequency of joint overuse injuries [6], relative to age-matched healthy individuals.

Multiple types of knee prostheses exist to help restore legged mobility to individuals with TFA [7, 8]. The most common are energetically passive prostheses, hereafter called passive prostheses. The two primary functions of a knee prosthesis are to support the user during the stance phase of walking and to provide appropriate lower leg motion during the swing phase. Passive prostheses provide support during stance phase (i.e., stance-knee stability) via a hyperextension stop which is engaged in stance phase by a combination of user hip torque and ground reaction force. In more advanced prostheses, stance-knee stability is supplemented via a modulated dissipater (e.g., a hydraulic damper with a controllable valve), which is typically engaged during stance phase (i.e., during load bearing) by microprocessor control (e.g., Otto Bock C-leg). This additional stance knee support, often called "stance control," improves the robustness of knee stability during the stance phase of walking, and also allows stance knee yielding during slope and stair descent. Types of knees which offer this stance control are called stance-controlled microprocessor-controlled knees (SCMPKs).

Swing phase is achieved in SCMPKs via inertial coupling between the double-pendulum of the thigh and shank (i.e., forward acceleration of the thigh drives initial knee flexion, while deceleration of the thigh drives subsequently knee extension). A small amount of damping at the knee (relative to the level of stance damping employed in stance-controlled knees) limits excessive knee flexion during swing and avoids terminal impact at full knee extension. One of the substantial benefits of the inertial coupling-based swing-phase movement of passive knee prostheses is that the movement of the knee is naturally and fundamentally coordinated with the movement and intent of the wearer. The same property that enables this natural coordination, however, also makes the swing-phase movement highly-susceptible to perturbations. Specifically, the same low impedance characteristic that enables the wearer to generate swing-phase motion, also environmental disturbances, such as stumble or scuff, to substantially influence the movement of the knee. Stance-knee stability relies on full extension at terminal swing, and thus, lack of robustness in swing phase jeopardizes stance-knee stability.

As an alternative approach to passive prostheses, several researchers have recently been exploring the potential merits of powered knee prostheses, as described in [9-18]. Powered knee prostheses typically provide both stance-phase support and swing phase motion using powered actuation at the knee. Such prostheses offer powered knee extension during stance phase, which can supplement or reduce hip effort during activities such as stair and slope ascent [19-21]. Additionally, in swing phase, powered knees are able to drive the knee movement along a specific trajectory, thus providing increased robustness of swing-phase motion relative to passive prostheses.

Although powered prostheses offer some functional advantages relative to passive devices, they also entail tradeoffs. Among these trade-offs are increased size, weight, and/or audible noise (relative to passive prostheses). Additionally, due to their use of large motors and transmissions, powered prostheses are characterized by high joint impedance in the powered mode, which changes the nature of interaction between a wearer and the device. As previously described, passive prostheses entail a low output impedance during swing, which enables the wearer to drive swing-phase motion such that the motion is fundamentally coordinated with the movement and intent of the wearer. When ambulating with a powered knee prosthesis, the user is less able to influence knee motion due to the high output impedance of the powered knee joint. As such, the movement of the device must be artificially coordinated with the movement and intent of the wearer, and consequently, there is no guarantee that this coordination is achieved.

The prosthesis design and control approach presented here is motivated by a recognition that SCMPKs have several desirable characteristics for the wearer including quiet operation, low weight, high support during stance, and an inertially-initiated swing phase. A number of studies validate the efficacy and value of SCMPKs for individuals with TFA, including [22-32]. For reasons previously stated, however, SCMPKs are also highly susceptible to swing-phase perturbations, which contribute to the high rate of falling in this population [4, 33, 34]. Specifically, falls generally occur as a result of stance-knee instability caused by failure of the knee to reach full extension at terminal swing. The low output impedance of the knee during swing phase in passive prostheses, which enables inertiallyinitiated swing phase, also results in poor disturbance rejection from external perturbations (e.g., scuffing). This susceptibility to perturbations is exacerbated by the inability of the device to provide the active power required to recover from such perturbations. Thus, although SCMPKs have been shown to provide effective mobility to individuals with TFA, they lack swing-phase robustness, which makes individuals with TFA more susceptible to falls.

The prosthesis described here is intended to retain the desirable characteristics and proven value of an SCMPK and improve upon them by enhancing the robustness of swing. Enhanced robustness during swing will better ensure full knee extension at terminal swing and thus increase stance-phase knee stability. This increased stability will presumably reduce the likelihood of falls. In order to enhance swing phase robustness, the authors propose to supplement an SCMPK using a small motor with a low-transmission ratio capable of implementing closed-loop control around swing phase without notably increasing knee impedance. The prosthesis is intended to provide stance and swing phase behavior in the same manner as an SCMPK, but with enhanced swing-phase robustness due to the powered closed loop, which is intended to better ensure full knee extension at terminal swing.

In order to achieve these functional aims, the prosthesis must be capable of providing a wide dynamic range of damping (i.e., low-impedance damping required for inertially-driven swing and high-impedance damping required for stance control); must employ a powered closed-loop control system that maintains the low-impedance associated with swing phase while in the powered state; and must be capable of switching between the low and high impedance states quickly at heel strike and heel off. The authors call this approach of supplementing an SCMPK with low-impedance power a stance-controlled swingassist (SCSA) prosthesis. Although a number of other powered, semi-powered, and/or hybrid prostheses have been proposed [9-18, 35-37], none provide, or has been shown to provide, the combination of behaviors necessary to implement the SCSA approach described here. This paper describes the design of an SCSA prosthesis, describes a walking controller for the prosthesis, and presents experimental results from testing on a TFA subject that demonstrates the behavior and potential merit of the prosthesis during both unperturbed and perturbed levelground walking.

II. DESIGN REQUIREMENTS

A. Size and Weight

The proposed prosthesis is intended to provide similar behavior to an SCMPK, but to do so with substantially increased robustness to swing-phase perturbations. This added robustness should not entail undue added mass or size relative to other SCMPKs. Two well-established SCMPKs are the Otto Bock C-Leg 4 and the Otto Bock Genium X3, which (with respective load cells) have a mass of 1.5 and 2.0 kg, respectively, and therefore have an average mass of 1.75 kg. Although one cannot state with specificity how the value added by increased swing phase robustness should trade with mass, the authors assume that an additional mass of 25% is a reasonable design target. As such, a design specification target mass of 2.2 kg was adopted. With regard to size, the C-Leg 4 measures approximately 310 mm. As such, the design target for the SCSA knee is 300 mm, which would result in a comparable length. Finally, to enable kneeling and sitting, the range of motion (ROM) target for the knee prototype should be at least 100 deg flexion and 5 deg hyperextension (i.e., total ROM of 105 deg).

B. Mechanical Power Dissipation Requirements

As previously stated, the design goal is to maintain the nominal swing and stance characteristics of an SCMPK. Since the passive torque, power, and damping values for such prostheses are not generally published, requirements for the modulated passive damping system were derived based on the quasi damping values present in healthy data during a range of activities, such as those given in [38-39]. Given these data, peak requirements for stance-knee yielding are associated with stair descent, which is characterized by a maximum resistive torque of 1.35 Nm/kg body mass, a maximum dissipative power of 4 W/kg, and a damping constant of approximately 1 Nm-s/rad-kg body mass, at a knee flexion angle of approximately 60 deg. Since the prototype is designed to accommodate users of at least 100 kg, the knee should therefore provide a peak resistive torque of at least 135 Nm, power dissipation of 400 W, and a maximum damping constant of at least 100 Nm-s/rad.

In addition to the stance phase requirements associated with knee yielding, the knee must also provide the low damping values associated with swing phase movement. Analyses of knee damping during swing phase based on data of healthy individuals indicates a damping constant of approximately 1 Nm-s/rad [38]. Therefore, in order to provide the essential SCMPK behaviors, a device should provide controllable damping between 1 Nm-s/rad to 100 Nm-s/rad, and must also be capable of switching between these extremes during heel strike and heel-off (i.e., characteristic time of switching on the order of 10 ms).

C. Power Generation Requirements

In addition to providing the essential behaviors of an SCMPK, the SCSA prosthesis also includes the swing-assist function. Preliminary work investigating a swing-assist prototype [40] indicated effective perturbation robustness could be achieved with peak active torques of 4 Nm flexion and 5.5 Nm in extension. Unlike the prototype reported in [40], which

does not include hydraulic stance control, the device presented here will have to overcome slight hydraulic damping and will likely have more rotational inertia. As such, the authors determined the swing-assist system should be designed to be able to provide a minimum of 7.5 Nm during swing, at a knee angular velocity of approximately 400 deg/s (7 rad/s), which corresponds to fast walking [38], and also corresponds to a requisite power generation of approximately 50 W. Finally, the knee must maintain a low swing-phase impedance (i.e., 1 Nm-s/rad) in the presence of powered assistance, such that the beneficial characteristics of an inertially-coupled swing-phase are retained.

D. Load Cell Requirements

For purposes of reliable stance control, and to transition to swing from late stance, the SCSA prosthesis requires a robust method of detecting both heel strike and toe off during various activities. In order to do so, the authors determined that axial force should be isolated from bending moment, such that application or removal of an axial load of 50 N could be detected independent of the sagittal plane moment present in the shank during the stance phase. Such moments can reach 150 Nm, depending on body mass and location within the shank [41].

E. Battery Life

The prototype should be battery-powered, with sufficient energy for at least one day of walking for the average user (2300 \pm 1500 steps) on a single charge [42]. In addition to providing sufficient energy for a day of use, the battery voltage and current capacities must enable the torque and speed requirements previously stated.

F. Summary of Design Specifications

A summary of the design specifications is as follows:

- Maximum power dissipation of 400 W.
- Assistive power generation of 50 W.
- Resistive knee torque up to 135 Nm.
- Assistive knee torque up to 7.5 Nm.
- Minimum swing-phase damping of 1 Nm-s/rad while in powered state.
- Maximum stance-phase damping of 100 Nm-s/rad.
- Ability to switch between damping extremes within 25 ms.
- Range of motion at least 100 deg flexion, 5 extension.
- Length target of 300 mm.
- Mass target of 2.2 kg.
- 50 N load sensing under applied moment conditions at heel strike and heel off.

III. DESIGN AND FABRICATION

A. Hybrid Actuator

As is the case with the C-leg devices, a closed-circuit hydraulic system was employed to achieve the relatively large torque, damping, and power dissipation specifications associated with stance-knee yielding, in addition to the relatively small torque, damping, and powered dissipation associated with swing-phase motion. Such an approach has

been shown to be provide the requisite torque and power, dynamic range of damping, and speed of switching for effective prosthesis performance, in a sufficiently compact and quiet package. The hydraulic system was supplemented with a relatively small electric motor coupled to the hydraulic system through a relatively low-ratio backdrivable transmission as implemented in previous work [43,44]. This motor enabled the supplementation of the low-impedance swing-phase with powered assistance. The components and layout of this hybrid actuator are depicted schematically in Fig. 1. Note that use of a linear (rather than rotary) hydraulic actuator enables use of higher hydraulic pressures, enabled by the improved sealing characteristics of sliding seals. The linear actuator was employed in a slider-crank configuration within the knee prosthesis. The geometry of the slider-crank was selected based on a weighted optimization that minimized the design envelope for the desired transmission ratio and minimized the variation in transmission ratio across the range of motion associated with level walking. The resulting transmission ratio is shown in Fig.

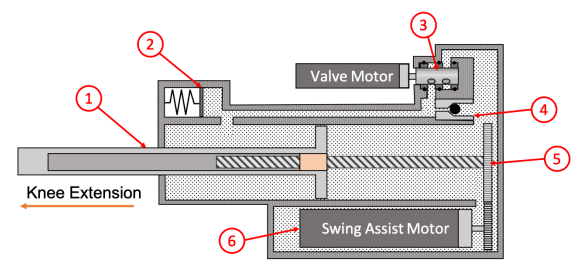


Fig. 1. Schematic of hybrid actuator, including: (1) a single rod cylinder with lead screw contained within rod; (2) spring-loaded accumulator biased toward extension; (3) rotary spool valve; (4) check valve allows for low-resistance extension; (5) lead screw and gear train driven by (6) a brushless motor.

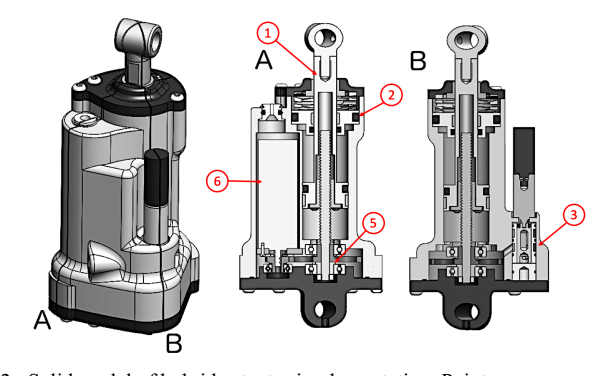


Fig. 2. Solid model of hybrid actuator implementation. Pointers correspond to items in Fig. 1. The check valve is not visible, since it is out of plane with the valve and drive systems.

The hybrid actuator, which consists of the combined hydraulic and electric subsystems, is shown in solid-model form in Fig. 2. For the hydraulic system, damping is modulated via a pressure-balanced rotary spool valve, which is actuated by a 12 mm diameter brushless gearmotor (Faulhaber 1226 with 64:1 gearhead). Since the high damping ratios required for stance phase are exclusively used to resist flexion, a check valve is employed in parallel with the rotary spool valve so that damping resistance to knee extension always remains low, even in cases that resistance to knee flexion is high. The main

hydraulic cylinder is a single-rod-type, which includes a spring-loaded accumulator to account for rod volume. The spring-loaded accumulator acts as a passive extension aid, and also increases the maximum achievable extension torque. The accumulator spring is a wave spring with a spring constant of 300 N/cm (166 lb/in), which at full flexion imposes a force of 160 N (35 lbs) on the accumulator piston, which generates a fluid pressure that provides an extension force of approximately 25 N on the main cylinder piston. This extension force, when acting through the cylinder-to-knee transmission ratio shown in Fig. 3, applies approximately 0.5 Nm of extension torque at the knee. Although the active power generation system is intended to replace a passive extension aid, presence of the passive aid is useful in the event of a power failure.

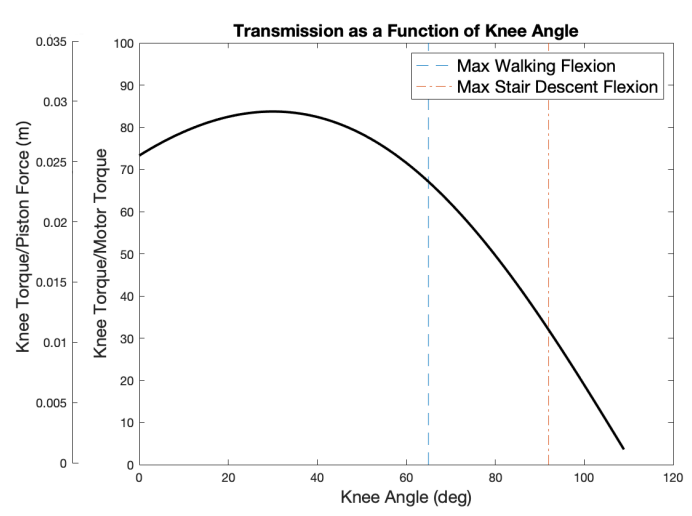


Fig. 3. Transmission ratio from cylinder to knee and swing-assist motor to knee as a function of knee flexion angle.

The hydraulic cylinder employs a one-inch diameter bore, which results in an estimated maximum pressure of 11.4 MPa (1660 psi) for an individual weighing 100 kg in stair descent. In order to minimize friction, the cylinder employs wear rings and cup seals along sliding surfaces, and O-rings or face seals at static interfaces.

In order to provide the assistive power requirements previously stated, a 90 W brushless motor was selected (Maxon EC22 90 W). The motor is rated at a maximum continuous torque of 50 mNm, and with proper heat-sinking, can be reasonably operated at a lower duty cycle to 150 mNm. As shown in Figs. 1 and 2, the motor is coupled to the hydraulic rod through a low-ratio and low-torque transmission, which consists of a lead screw located within the piston rod, driven by the motor through a pair of spur gears. The combined rotary-tolinear transmission ratio is approximately 3050 rad/m, which, in combination with the previously described slider-crank configuration, provides a rotational transmission ratio between the electric motor and knee as shown in Fig. 3 (i.e., nominally 75:1 within the typical walking range of motion). Given this transmission, the motor will provide approximately 9 Nm of knee torque (under ideal circumstances). Alternatively, assuming an 85% transmission ratio efficiency, the motor will provide 7.5 Nm of active torque and approximately 75 W of active power at the knee. Note that in the same way as the actuators designed in [43-45], the entire system is submerged in oil, which is intended to reduce friction in the gears and lead screw and therefore minimize backdrive friction (i.e., minimize output impedance). As indicated in Figs. 1 and 2, the motor is also flooded in the same oil. In cases in which the oil temperature is expected to remain low (e.g., level walking), the oil will improve peak torque and power characteristics of the motor; in cases of oil heating, however, such as during extended periods of stair descent, the oil may limit the performance of the motor drive subsystem.

B. Load Cell

As previously stated, the load cell should measure axial force within a range of zero to 50 N and should withstand up to 150 Nm of moment. The authors are unaware of any commerciallyavailable load cell that meets these measurement specifications, particularly within the size and weight constraints associated with this prosthesis. In order to decrease sensitivity to moment, the authors constructed a load cell as depicted schematically and in solid-model form in cross-section in Fig. 4. The load cell employs a set of custom linear bearings to isolate axial from bending loads in the shank. In order to maximize spatial efficiency, the load cell was designed to also serve as a pylon clamp, such that the vertical space occupied by the load cell would not add to the overall length of the prosthesis. The races of the custom linear ball bearings were fabricated from posthardened A2 tool steel, which employ non-circulating bearing balls of 3/32" in) diameter.

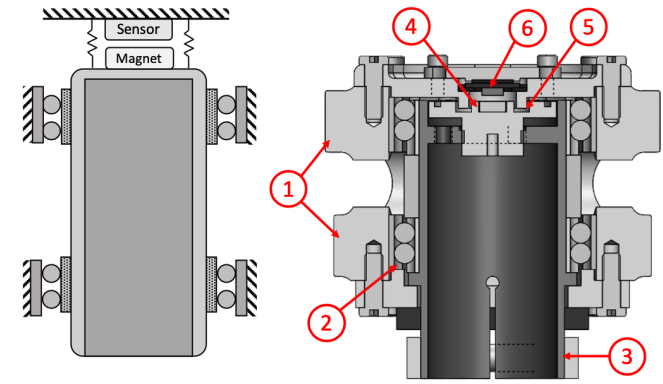


Fig. 4. Schematic and solid model cross-section of load cell. The load cell is design around a pylon clamp (3) which translates vertically. Bending moments are reacted by custom linear ball bearings (2) which are coaxial with the pylon clamp. A Hall Effect sensor (6) is used in conjunction with a magnet (4) to detect deformation in a wave spring (5). The assembly is held into the knee housing by locating extrusions on its sides (1).

Given the use of linear bearings to isolate axial movement from bending moments, the axial load is measured by employing a spring stack in combination with a magnet and magnetic field sensor (Fig. 4). The spring constant of the stack is 5870 N/cm (3300 lb/inch). Since the load cell is intended to detect heel strike and toe-off, rather than peak loads, the spring stack saturates at a load of approximately 170 N (40 lb), which limits load cell deflection to approximately 1.4 mm (0.06 in).

C. Housing and Complete Mechanical Assembly

The knee housing was designed in two halves with the main

components - the hybrid actuator and the load cell - located between them. Figure 5 shows the prosthesis with one housing side removed, showing the position of the actuator and load cell within the housing. Figure 5 also shows the fully assembled knee housing, showing the location of the embedded system and battery pack. Contact between the housing and rotational assembly (i.e., crank) provides hard stops in both extension and flexion. The total range of motion of the knee is 130 deg (5 deg hyperextension to 125 deg flexion). Note that, as indicated in Fig. 3, the actuator reaches a singularity at 110 deg flexion, such that movement between 110 deg and 125 deg flexion is nonactuated. The length of the prosthesis from the mounting location of the socket to the base of the pylon clamp measures 278 mm. The mass of each component is listed in Table I. The total mass of the assembled prosthesis, filled with hydraulic fluid, is 2180 g. Note that the housing was constructed from magnesium alloy (AZ31B-H24), aided by finite element analyses, which helped reduce mass relative to aluminum alloy.

TABLE I MASS DISTRIBUTION

Component	Mass (g)
Housing	430
Rotary crank assembly	175
Actuator	910
Load cell assembly	385
Embedded system	30
Battery pack	135
ABS covers, screws, misc.	115
Total Mass	2180

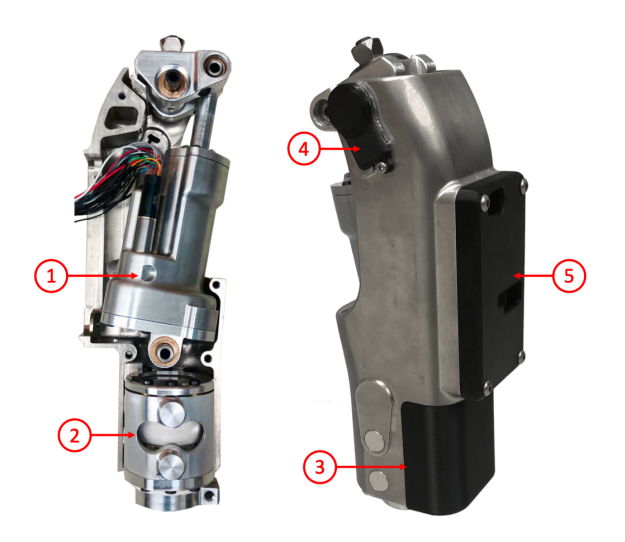


Fig. 5. Knee prosthesis prototype with one half of the housing removed (left), displaying the linear actuator (1) and the load cell (2) in their assembled positions. Fully assembled knee prosthesis prototype (right), including black ABS covers that house the battery pack (3), absolute encoder (4), and embedded system (5).

D. Embedded System

A custom embedded system, shown in Fig. 6, was designed to provide sensing, actuation, and control of the prosthesis. The embedded system includes: 1) two custom brushless motor drivers with closed-loop current control; 2) sensing and signal conditioning including absolute angle sensing at the knee joint which is fused with high-resolution incremental angle sensing

at the drive motor, incremental angle sensing at the valve motor, axial force load measurement, and a six-axis inertial measurement unit; 3) two microcontrollers for high and low level control; 4) SD card for data storage; and 5) CAN communication hardware for interfacing with other control systems. The brushless motor control and encoder processing is provided via a Microchip digital signal processor (DSPIC33FJ64GS608-50I/PT), which communicates via SPI with a 32-bit general-purpose microcontroller (Microchip PIC32 MZ2048EFM100-I/PF), which runs higher-level control functions and interfaces with the IMU, load cell sensor, absolute encoder, SD card, and CAN bus. The PIC32 runs servo control loops around each motor at a 1 kHz sampling rate, passing a desired torque value to the dsPIC, which runs each respective (PI) current control loop at approximately 5.6 kHz. The dsPIC then outputs PWM signals (at approximately 98 kHz) to the appropriate MOSFETS of custom brushless motor drivers to drive the respective motors. The system is powered using three 18650 batteries (INR18650-30Q) in series, providing nominal 12.6 V and 36 W-hrs at full charge, with a maximum continuous current capacity of 15 A. Preliminary research using a swing-assist prototype required on average 6 W of active power for level walking. At this rate, the batteries used in this prototype would provide for 6 hrs of continuous walking, or approximately 36,000 steps of walking between charges.





Fig. 6. Top and bottom view of embedded system. The board measures 115 mm long by 60 mm wide.

IV. BENCHTOP SUBSYSTEM TESTING

A. Modulated Hydraulic Subsystem

To validate that the hydraulic system provides the desired range of damping, an instrumented press was used to cycle the hydraulic cylinder through compression and extension while force-velocity data was recorded. This testing was performed with the rotary spool valve in several predetermined orientations, ranging from fully open to fully closed (approximately 65 deg of spool motion). Figure 7 shows the experimental results. As can be seen in the figure, variation in spool valve changes the level of hydraulic damping

substantially in flexion. Due to the presence of the check valve, however, the actuator provides the same, relatively low level of damping in extension, regardless of spool valve setting. The damping in flexion for the valve fully open corresponds to a linear damping of 6 N-s/cm, while the damping with the valve fully closed corresponds to 190,000 N-s/cm. The damping in extension corresponds to approximately 4 N-s/cm (regardless of valve position). Recall that the design specifications require a dynamic range of damping between 1 Nm-s and 100 Nm-s. Rendering these values in the linear actuator space (i.e., via the square of the transmission ratio shown in Fig. 3) indicates a required damping range between 23 and 3900 N-s/cm (the latter is shown as a solid line in Fig. 7). As such, the hydraulic actuator provides a dynamic range that exceeds that required of the knee prosthesis.

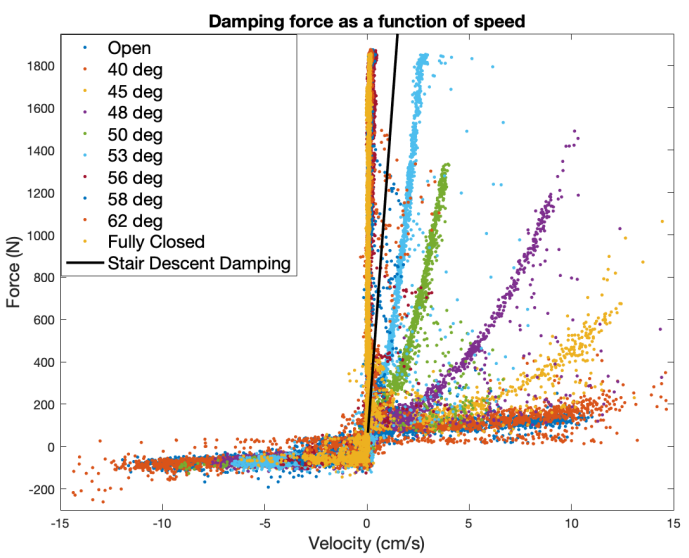


Fig. 7. Damping characteristics of hydraulic actuator as a function of valve position. The damping can be varied from 6 to 19,000 N-s/cm when resisting retraction, and due to the check valve, maintains an approximately constant damping coefficient of 3.85 N-s/cm when resisting extension.

B. Motor Drive Subsystem

The motor drive system is intended to supplement and provide perturbation robustness around a nominally-passive swingphase motion, rather than to provide a high-impedance fullypowered swing motion. As an initial validation of the active drive system, the knee prosthesis was commanded to track a trajectory while suspended by the (proximal) pyramid joint and configured with a pylon and 28 cm carbon-fiber foot prosthesis (Freedom Pacifica). Figure 8 shows command tracking of a 1 Hz sinusoid where zero angle corresponds to the shank being aligned with the vertical. The hydraulic spool valve was fully open, and the supplied current was externally limited to 6 A in order to avoid damage to the windings, since overheating safeguards were not yet implemented. As indicated in the figure, the active drive system is capable of providing closedloop movement assistance at movement frequencies representative of swing-phase movement during walking. A video of these tests is provided in the supplemental material. The video also qualitatively demonstrates the output impedance of the knee during swing phase (i.e., shown with the motor drive subsystem being back-driven).

The sound level was measured with a sound level meter during the 1 Hz sinusoidal tracking. At a distance of one meter, the sound level was 46 dBA, which is approximately an order of magnitude quieter (in terms of sound power) than a fully-powered prosthesis previously developed by the authors [46].

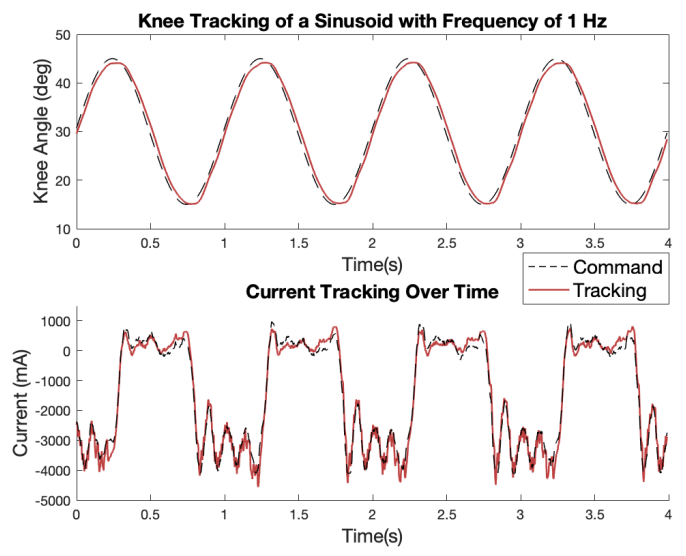


Fig. 8. Sinusoidal tracking of a 1 Hz sine command, and corresponding current/torque tracking associated with servo controller.

V. WALKING CONTROLLER

A finite-state walking controller was developed for the SCSA knee to support walking with enhanced robustness to swingphase perturbations. The walking controller is comprised of four states: 1) Stance (ST); 2) Pre-swing (PS); 3) Swing flexion (SF); and 4) Swing extension (SE). Note that the PS occurs during late stance. In normal walking, the controller cycles sequentially through these states, moving between sequential states based on the combination of conditions outlined in Table II, all of which are based on real-time measurements provided by the IMU, knee angle sensing, and/or the load cell. The prosthesis is configured within each state as follows. In the ST state, the rotary spool valve in the hydraulic subsystem is closed, which precludes flexion of the knee, while the motor drive subsystem remains inactive. In the PS state, the rotary spool valve is opened to allow the user to initiate swing phase, while the motor drive subsystem remains inactive. As the controller switches into the SF state, a cadence-adaptive splinebased swing-phase trajectory is generated, based on similar methods described in [46], and a PD controller is employed in the motor drive subsystem to track this desired trajectory. When the controller switches into the SE state, the motor drive subsystem continues to track the desired trajectory, while the hydraulic spool valve is moved to the closed position. Note that doing so does not interfere with swing extension, since the hydraulic fluid during swing extension flows exclusively through the check valve (see Fig. 1). Following the SE state, the motor-drive subsystem is turned off, allowing the hydraulic stance control system to provide stance knee stability.

TABLE II. WALKING CONTROLLER STATE TRANSITIONS:
POSITIVE ANGLES AND VELOCITIES INDICATE JOINT FLEXION
AND/OR LIMB FORWARD OF WEARER.

Transition	Condition	
ST to PS	Thigh angle < -5 deg	
PS to SF	Thigh angular velocity > 0 or Force < 50 N	
SF to SE	Knee angular velocity < -5 rad/s	
SE to ST	Knee angle < 0 or Force > 50 N	

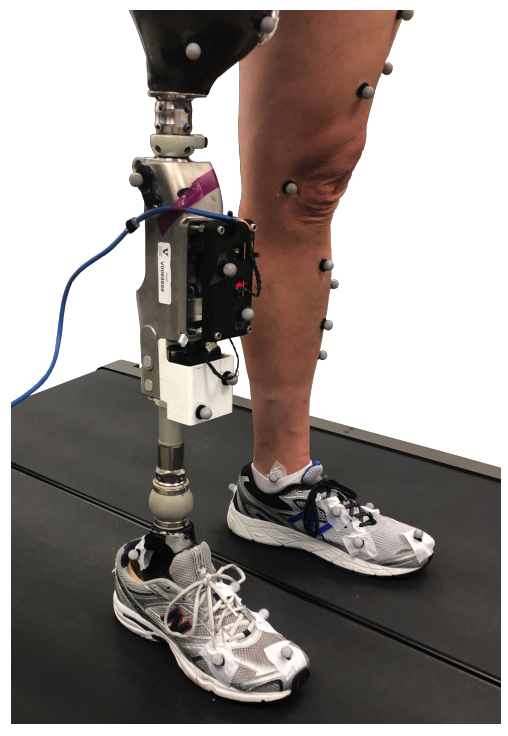


Fig. 9. Subject with transfemoral amputation wearing SCSA prosthesis prototype, in addition to motion capture markers employed in data collection.

VI. HUMAN SUBJECT TESTING

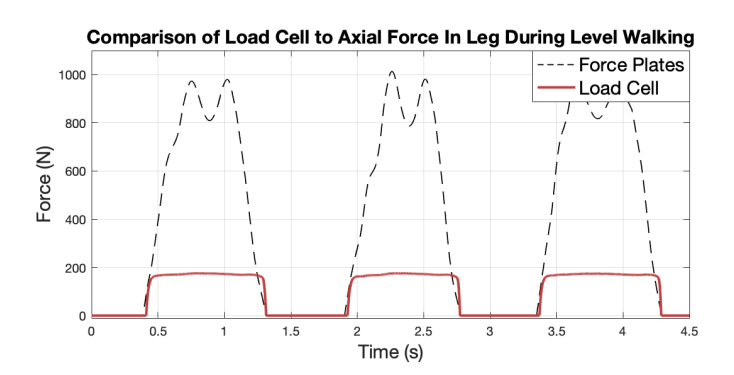
The walking controller was implemented in the SCSA prosthesis prototype (with switching conditions given in Table II), and the prosthesis was tested with IRB approval on a single subject (male 6'3", 217 lb) with transfemoral amputation. In these tests, the subject walked on a split-belt, forceinstrumented treadmill (Bertec, Columbus, USA), while fullbody kinematic data were collected via an infrared motion capture system (Vicon, Oxford, GBR), as shown in Fig. 9. The integrated motion capture and force plate system, in combination with Visual3D inverse dynamics-based software (C-Motion, Germantown, USA), provided measurement of prosthesis knee angle and ground reaction force, in addition to the prosthesis side hip torque and power. Two types of experiments were performed: non-perturbed walking and perturbed walking tests. In both types of tests, the subject performed the test first with his daily-use prosthesis, which was a microprocessor-controlled energetically passive knee (Rheo Knee, Ossur), and subsequently with the SCSA prototype knee.

A. Treadmill Walking Tests

In the first set of tests, the subject walked for a period of 90 s at a treadmill speed of 0.8 m/s while data was recorded. The treadmill speed of 0.8 m/s was selected by the subject as a

comfortable speed while walking on his daily-use prosthesis. Following that testing, the subject was fit with the SCSA prosthesis prototype and allowed to accommodate to the prosthesis during first over-ground walking, and subsequently during treadmill walking. Following this period of acclimation (approximately 30-60 min total), the subject walked for 90 s at the same treadmill speed while data was recorded.

The top plot in Fig. 10 shows axial force data (i.e., force along the shank) during three representative strides while walking on the SCSA prototype during the steady-state walking trials, as measured by: 1) the force plate in combination with the motion capture instrumentation, and 2) the SCSA load cell described in section III.B. The figure also shows clearly the load cell saturation at approximately 170 N, as described in section III.B. The bottom plot in Fig. 10 shows sagittal plane ankle torque, knee torque, and load cell torque as measured by the laboratory instrumentation, for the same three strides, characterizing the substantial sagittal-plane moments to which the load cell is subjected during stance.



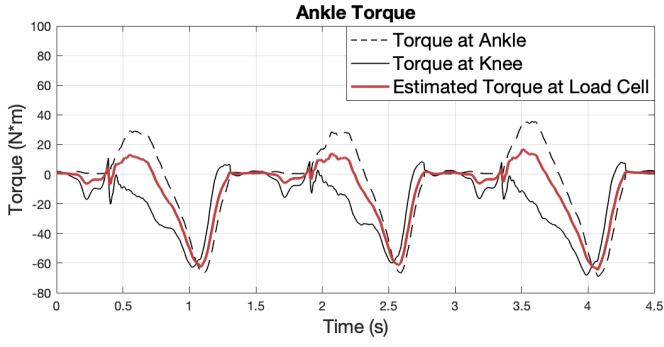


Fig. 10. (TOP) Force plate and load cell measurements during treadmill walking, and (BOTTOM) corresponding ankle torque

Figure 11 shows comparative data for both the SCSA prototype and daily-use prostheses corresponding to the steady-state walking trials. The figures shows mean data as a function of stride over approximately 70 strides for each prosthesis, along with bands that represent a standard deviation about the mean. The top plot shows knee angle for both prostheses, indicating a mean peak knee flexion angle of 60 deg for the SCSA knee, and 50 deg for the daily-use prosthesis. The middle plot shows hip torque for both prostheses. The torque corresponding to the daily-use prosthesis is characterized by an RMS value of 28.0 Nm, while the RMS torque corresponding to the SCSA prosthesis was 24.1 Nm. The bottom plot shows hip power for this single subject for each prosthesis condition, characterized by an RMS value of 30.2 W for the daily-use, and

27.3 W for the SCSA. Two sample t-tests were used to verify differences in means, which in both cases were significant with p<0.01. Video of the corresponding walking trials is included in the supplemental material.

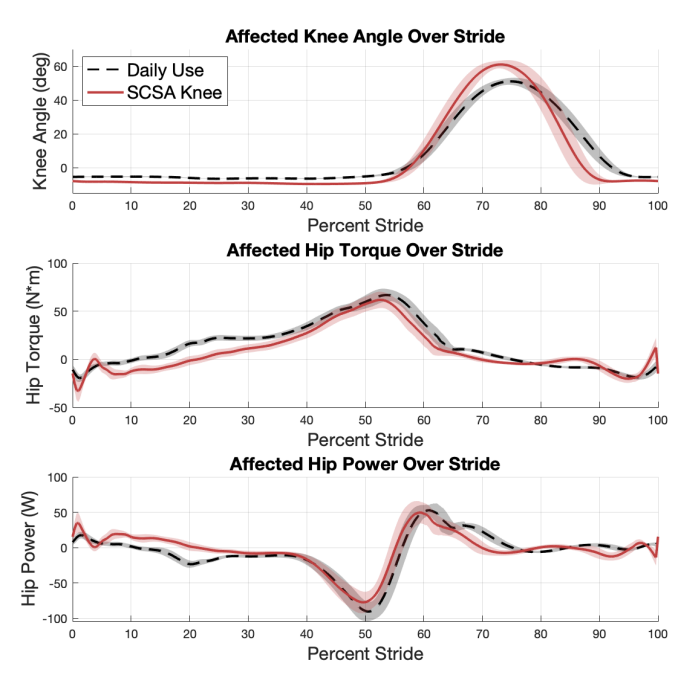


Fig. 11. Mean knee angle, hip torque, and hip power for the SCSA and dailyuse prostheses, respectively, and one standard deviation about the mean during level treadmill walking.

B. Scuff-type Walking Perturbation

In addition to testing knee behavior during normal walking, the ability of each prosthesis to respond to a swing-phase disturbance was tested by introducing a scuff perturbation object to the treadmill during a second set of walking trials. The perturbation apparatus, described in a recent publication [47], introduced a small steel wedge, approximately 1 cm in height, to the treadmill to induce a scuff response. As part of this experiment, the subject wore glasses to occlude peripheral vision, sound-cancelling earphones, and also an overhead harness for safety. The perturbations were introduced by a computer-controlled timing system, as described in [47], at a consistent percentage of stride for both the daily-use prosthesis, and the SCSA prototype. The subject's knee angle during a representative scuff perturbation for both prostheses is shown in the top plot of Fig. 12, where the scuff perturbation occurs at approximately 2.1 s, as indicated in the figure by the dash-dot vertical line. As shown in the figure, following the scuff perturbation, the daily-use knee prosthesis flexes prior to eventually extending; in contrast, the SCSA knee prosthesis extends substantially faster. A video of both perturbation trials shown in Fig. 12 is included in the supplemental material and provides a better sense of whole-body movement during the respective scuff perturbations. The bottom plot of Fig. 12 shows the motor current, which is indicative of the motor torque, corresponding to the SCSA scuff perturbation trial. In the plot, positive current corresponds to an active extension torque at the knee. It is clear from the data that the scuff perturbation elicits a substantial reactive knee torque in the

extension direction following the perturbation, which results in the rapid knee extension seen in the knee response.

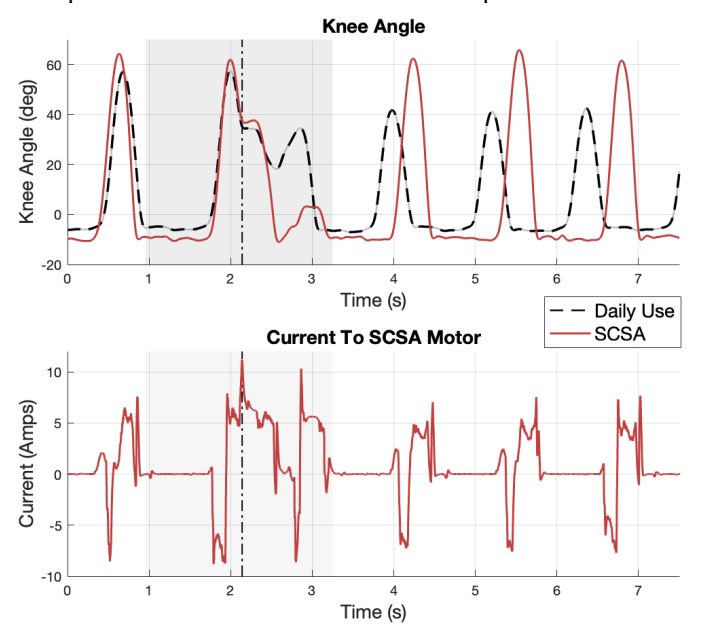


Fig. 12. Mean knee angle, hip torque, and hip power for the SCSA and dailyuse prostheses, respectively, and one standard deviation about the mean. Greyed out block represents the stride during which perturbation occurs

VII. DISCUSSION

A. SCSA Prototype Characteristics

The mass and length of the SCSA prototype are 2.2 kg and 28 cm, respectively. The knee range of motion is 130 deg. For the hydraulic subsystem, the data in Fig. 7 indicates an achievable range of damping that encompasses the range of 1 Nm-s/rad and 100 Nm-s/rad, shows resistive force equivalent to 60 Nm of knee torque, and dissipative power of 150 W. If operated at the rated maximum pressure, the hydraulic subsystem would provide more than the 135 Nm of torque and 400 W of power required. The efficiency of the motor-drive subsystem was measured at 88% by comparing the output torque of the system (measured via force gauge) to the expected torque based on knee configuration and motor current. As such, the SCSA prototype design meets, or would at its rated pressure meet, the design specifications enumerated in section II.F.

B. Trade-offs Relative to Other Prosthesis Types

The value proposition of the SCSA prosthesis is to offer to the user improved swing-phase characteristics relative to a stance-controlled energetically passive knee prosthesis, in exchange for a moderate increase in device mass. As characterized by [38] and others, healthy individuals exhibit approximately 60 deg peak knee flexion when walking at a self-selected speed. As shown in the data presented in Fig. 11, the SCSA prosthesis provides 60 deg of knee flexion, while the daily-use prosthesis provides approximately 50. As also measured during the same experiments, for the individual tested, the hip torque and power required while walking was reduced by the SCSA prosthesis by 14% and 10%, respectively, despite increased knee flexion and increased rotational inertia. While this data is not conclusive for

its effects on a broader population, it does show promising potential for more optimized gait.

In addition to offering potential benefits in level walking, the SCSA prosthesis is intended to improve robustness to swing-phase perturbations. As shown in Fig. 12, and perhaps to a greater extent in the video included in the supplemental material, the SCSA prosthesis appears to provide substantially improved robustness to swing-phase perturbations.

The SCSA prosthesis provides the aforementioned potential functional benefits at the expense of a moderate increase in device mass relative to passive devices. The daily-use knee prosthesis used in the experiments described here, the Ossur Rheo Knee, has a mass of 1.6 kg, lighter than the SCSA prototype, which has a mass of 2.2 kg. The SCSA knee therefore provides the aforementioned potential swing-phase benefits with a 37.5% increase in device mass relative to the passive knee.

VIII. CONCLUSION AND FUTURE WORK

This paper describes a new approach to knee prostheses that supplements an energetically passive SCMPK with a small, highly-backdrivable motor. In doing so, the approach is intended to retain the beneficial aspects of the SCMPK, including quiet operation and inertially-driven swing phase, but to substantially increase the robustness of swing-phase movement to perturbations. Although swing phase remains primarily inertially-driven, it is supplemented with a closedloop control system around swing phase motion, which acts to correct deviations from the nominal ballistic swing phase. Testing on an individual with TFA during unperturbed walking indicates increased knee flexion and decreased hip effort relative to an SCMPK. Further, testing during perturbed walking indicates a substantially faster recovery from the perturbation relative to the SCMPK. As such, the approach appears to provide the essential character of an SCMPK, while also providing enhanced swing-phase characteristics.

REFERENCES

- [1] K. Ziegler-Graham, E. MacKenzie, P. Ephraim, T. Travison and R. Brookmeyer, "Estimating the prevalence of limb loss in the United States: 2005 to 2050", Arch Phys Med Rehabil, vol. 89, no. 3, pp. 422-429, 2008.
- [2] T.R.Dillingham, L.E. Pezzin, E.J.MacKenzie, "Limb Amputation and Limb Deficiency: Epidemiology and Recent Trends in the United States", Southern Medical Journal, vol. 95, no. 8
- [3] R. Renzi, N. Unwin, R. Jubelirer and L. Haag, "An international comparison of lower extremity amputation rates", *Annals of Vascular Surgery*, vol. 20, no. 3, pp. 346-350, 2006.
- [4] C. Gauthier-Gagnon, M. C. Grise, and D. Potvin, "Enabling factors related to prosthetic use by people with transtibial and transfemoral amputation," *Arch Phys Med Rehabil*, vol. 80, no. 6, pp. 706-13, Jun, 1999.
- [5] L. A. Talbot, R. J. Musiol, E. K. Witham, and E. J. Metter, "Falls in young, middle-aged and older community dwelling adults: perceived cause, environmental factors and injury," *BMC Public Health*, vol. 5, pp. 86, 2005.
- [6] R. E. Seroussi, A. Gitter, J. M. Czerniecki, and K. Weaver, "Mechanical work adaptations of above-knee amputee ambulation," *Arch. Phys. Med. Rehabil.*, vol. 77, no. 11, pp. 1209–1214, 1996.
- [7] H. D. Romo, "Prosthetic knees," *Phys Med Rehabil Clin N Am*, vol. 11, no. 3, pp. 595–607, 2000.

- [8] R. E. Stewart, A. Staros. "Selection and application of knee mechanisms." Bulletin of prosthetics research, vol. 18, pp. 90-158, 1972.
- [9] M. Windrich, M. Grimmer, O. Christ, S. Rinderknecht, P. Beckerle, "Active lower limb prosthetics: a systematic review of design issues and solutions", *BioMedical Engineering OnLine*, vol. 15, no. 3, 2016.
- [10] F. Sup, H. A. Varol, J. Mitchell, T. J. Withrow, M. Goldfarb, "Preliminary evaluations of a self-contained anthropomorphic transfemoral prosthesis," *IEEE/ASME Trans. Mechatronics*, vol. 14, no. 6, pp. 667-676, Dec. 2009.
- [11] C. D. Hoover, G. D. Fulk, K. B. Fite, "The design and initial experimental validation of an active myoelectric transfemoral prosthesis," *J Med. Devices*, vol. 6, no. 1, pp. 011005, Mar. 2012.
- [12] M. Lui, P. Datseris, H. H. Huang, "A prototype for smart prosthetic legsanalysis and mechanical design," *Adv Mater Res.*, vols. 403-408, pp.1999-2006, 2012.
- [13] S. Pfeifer, R. Riener, H. Vallery, "An actuated transfemoral prosthesis with optimized polycentric knee joint," Presented at IEEE RAS & EMBS BioRob. New York; 2012. p. 1807–12.
- [14] L. Flynn, J. Geeroms, R. Jimenez-Fabian, B. Vanderborght, D. Lefeber, "CYBERLEGS beta-prosthesis active knee system," presented at the 2015 IEEE-ICORR, 2015, pp. 410-415.
- [15] G. Waycaster, S. K. Wu, X. R. Shen, "Design and control of a pneumatic artificial muscle actuated above-knee prosthesis," *J Med Devices*, vol. 5, no. 3, pp. 03103, Sep. 2011.
- [16] H. Zhao, E. Ambrose, A. D. Ames, "Preliminary results on energy efficient 3D prosthetic walking with a powered compliant transfemoral prosthesis," presented at the 2017 IEEE-ICRA, 2017, pp. 1140-7.
- [17] T. Elery, S. Rezazadeh, C. Nesler, J. Doan, H. Zhu, and R. D. Gregg, "Design and benchtop validation of a powered knee-ankle prosthesis with high-torque, low-impedance actuators," in Proc. IEEE Int. Conf. Robot. Autom., Brisbane, Australia, 2018, pp. 2788-2795.
- [18] A. F. Azocar, L. M. Mooney, L. J. Hargrove, E. J.Rouse, "Design and characterization of an open-source robotic leg prosthesis," 2018 7th IEEE – BioRob., Enschede, Netherlands, 2018, pp 111-118.
- [19] B. Lawson, H. A. Varol, A. Huff, E. Erdemir, and M. Goldfarb, "Control of stair ascent and descent with a powered transferoral prosthesis," IEEE Trans. Neural Syst. Rehabil. Eng., vol. 21, no. 3, pp. 466-473, 2013.
- [20] F. Sup, H. A. Varol, and M. Goldfarb, "Upslope walking with a powered knee and ankle prosthesis: initial results with an amputee subject," IEEE Trans Neural Syst. Rehabil. Eng., vol. 19, no. 1, pp. 71-8, Feb. 2011.
- [21] E.D. Ledoux, B.E. Lawson, A.H. Schultz, H.L. Bartlett, M. Goldfarb, "Metabolics of stair ascent with a powered transfemoral prosthesis," Published in 2015 IEEE EMBC Conference, 2015
- [22] B. J. Hafner, L. L. Willingham, N. C. Buell, K. J. Allyn, D. G. Smith, "Evaluation of function, performance, and preference as transfemoral amputees transition from mechanical to microprocessor control of the prosthetic knee," *Arch Phys Med Rehabil*, vol. 88, no. 2, pp. 207-17, Feb, 2007.
- [23] K.R. Kaufman, K.A. Bernhardt, K. Symms, "Functional assessment and satisfaction of transfemoral amputees with mobility (FASTK2: A clinical trial of microprocessor-controlled vs. non-microprocessor-controlled knees." Clin Biomech 58:116-122, 2018
- [24] A. Kannenberg, B. Zacharias, E. Pröbsting, "Benefits of microprocessor prosthetic knees to limited community ambulators: a systematic review." J Rehabil Res Dev,51:1469-1495, 2014
- [25] K. Wong, J. Rheinstein, M. A. Stern, "Benefits for adults with transfemoral amputation and peripheral artery disease using microprocessor compared with non microprocessor prosthetic knees." Arch Phys Med, 94:804-810, 2015
- [26] V.J. Eberly, S.J. Mulroy, J.K. Gronley, J. Perry, J.M.Burnfield, "Impact of a stance phase microprocessor-controlled knee prosthesis on level walking in lower functioning individuals with transfermoral amputation," *Prosth Orthot Int* 2014; 38(6):447-445
- [27] C.K. Wong, S. Benoy, W. Blackwell, S. Jones, R. Rahal, "A comparison of energy expenditure in people with transfemoral amputation using microprocessor and nonmicroprocessor knee prostheses: a systematic review," J Prosthet Orthot 2012; 24(4) 202-208
- [28] C.K. Wong, J. Wilska, M. Stern, "Balance, balance confidence, and falls using nonmicroprocessor and microprocessor knee prostheses: a case study after vascular amputation with 12-month follow-up," J Prosthet Orthot 2012; 24(1): 16-18
- [29] J.M. Burnfield, V.J. Eberly, J.K. Gronely, J. Perry, W.J. Yule, S.J. Mulroy, "Impact of stance phase microprocessor-controlled knee

- prosthesis on ramp negotiation and community walking function in K2 level transfemoral amputees," *Prosthet Orthot Int* 2012, 36(1):95-104
- [30] P. Theeven, B. Hemmen, F. Rings, G. Meys, P. Brink, R. Smeets, H. Seelen, "Functional added value of microprocessor-controlled knee joints in daily life performance of Medicare Functional Classification Level-2 amputees," J Rehabil Med 2011; 43(10):906-915
- [31] D. Berry, M.D. Olson, K. Larntz, "Perceived stability, function, and satisfaction among transferoral amputees using microprocessor and nonmicroprocessor controlled prosthetic knees: a multicenter survey," J Prosthet Orthot 2009, 21(1): 32-42
- [32] K.R. Kaufman, J.A. Levine, R.H. Brey, et al. "Gait and Balance of transfemoral amputees using passive mechanical and microprocessorcontrolled prosthetic knees," *Gait Posture* 2007; 26:489-493
- [33] W.C. Miller, A. B. Deathe, M. Speechley, J. Koval, "The invluence of falling, fear of falling, and balance confidence on prosthetic mobility and social activity among individuals with a lower extremity amputation," *Arch Phys Med Rehabil*, vol. 82, no. 9, pp. 1238-1244, Sep, 2001.
- [34] W.C. Miller, A. B. Deathe, M. Speechley, "Lower extremity prosthetic mobility: A comparison of 3 self-reported scales," *Arch Phys Med Rehabil*, vol. 82, no. 10, pp. 1432-1440, Oct, 2001.
- [35] E. Rouse, L. Mooney and H. Herr, "Clutchable series-elastic actuator: implications for prosthetic knee design", *The International Journal of Robotics Research*, vol. 33, no. 13, pp. 1611-1625, 2014.
- [36] T. Lenzi, M. Cempini, L. Hargrove, T. Kuiken, "Design, development, and testing of a lightweight hybrid robotic knee prosthesis," *The International Journal of Robotics Research*, vol. 37, pp. 953-976, July 2018
- [37] B. Lambrecht and H. Kazerooni, "Design of a semi-active knee prosthesis", Presented at 2009 IEEE-ICRA, 2009, pp. 639-45.
- [38] D. A. Winter, Biomechanics and Motor Control of Human Gait: Normal, Elderly and Pathological, 1991.
- [39] R. Riener, M. Rabuffetti, and C. Frigo, "Stair ascent and descent at different inclinations," *Gait & posture*, vol. 15, pp. 32-44, 2002.
- [40] A. Baimyshev, B. Lawson, M. Goldfarb, "Design and assessment of lightweight swing-assist knee prosthesis," Presented at 2018 IEEE-IMBC 2018
- [41] Johansson et al., "A Clinical Comparison of Variable Damping and Mechanically Passive Prosthetic Knee Devices", American Journal of Physical Medicine and Rehabilitation, vol 84, issue 8, pp 563-575
- [42] J. M. Stepien, S. Cavenett, L. Taylor, M. Crotty, "Activity levels among lower-limb amputees: self-report versus step activity monitor," *Arch Phys Med Rehabil.*, vol. 88, no. 7, pp. 896-900, July 2007.
- [43] H. Bartlett, B. Lawson, M. Goldfarb, "Design of a power-asymmetric actuator for a transtibial prosthesis," Presented at 2017 IEEE-ICORR, 2017, pp. 1531-36
- [44] H.L. Bartlett, B.E. Lawson, M. Goldfarb, "Design, Control, and Preliminary Assessment of a Multifunctional Semipowered Ankle Prosthesis", IEEE Trans Mech, vol. 24, Issue 4, Aug. 2019
- [45] T. Yu, A.R. Plummer, P. Iravani, J. Bhatti, S. Zahedi, D. Moser, "The Design, Control, and Testing of Integrated Electrohydrostatic Powered Ankle Prosthesis," IEEE Trans Mech, vol. 24, Issue 3, June 2019
- [46] B. Lawson et al., "A Robotic Leg Prosthesis: Design, Control and Implementation", IEEE Robotics and Automation Magazine, vol. 21, Issue 4
- [47] S.T. King, M.E. Eveld, A. Martinez, K. Zelik, M. Goldfarb, "Development of a Novel Gait Perturbation System for the Study of Stumble Recovery", Journal of NeuroEngineering and Rehabilitation, 2019. in press.



Jantzen Lee (S'18) received the B.S. degree in mechanical engineering from Auburn University in Auburn, Alabama in 2017. From 2017 to present, he has been a Research Assistant at the University of Vanderbilt, specializing in mechanical and embedded system design.



Harrison Logan Bartlett (S'16) received the B.S. degree in biomedical engineering from the Georgia Institute of Technology, Atlanta, GA, USA, in 2014 and the M.S. and Ph.D. degrees in mechanical engineering from Vanderbilt University, Nashville, TN, USA, in 2018. Currently, he is a Research Engineer at Vanderbilt University, Nashville, TN. His research

interests include the mechanical design and control of rehabilitation robotic devices with an emphasis on powered and semi-powered lower limb prostheses.



Michael Goldfarb (S'93–M'95) received the B.S. degree in mechanical engineering from the University of Arizona in 1988, and the S.M. and Ph.D. degrees in mechanical engineering from MIT in 1992 and 1994. Since 1994, he has been at Vanderbilt University, where he is currently the H. Fort Flowers Professor of

Mechanical Engineering, Professor of Electrical Engineering, and Professor of Physical Medicine and Rehabilitation. His research interest is the design and control of robotic systems that interact physically with people, with a particular focus on the development of assistive devices to improve quality of life for people with physical disabilities.